JARO 15: 13–30 (2014)
DOI: 10.1007/s10162-013-0425-9

JARO
Journal of the Association for Research in Otolaryngology

Research Article

Permeation of Fluorophore-Conjugated Phalloidin into Live Hair Cells of the Inner Ear Is Modulated by P2Y Receptors

Benjamin R. Thiede[1] and Jeffrey T. Corwin[1,2]

[1]*Department of Neuroscience, University of Virginia School of Medicine, 409 Lane Rd, PO Box 801392, Charlottesville, VA 22908, USA*
[2]*Department of Cell Biology, University of Virginia School of Medicine, Charlottesville, VA 22908, USA*

Received: 22 July 2013; Accepted: 23 October 2013; Online publication: 22 November 2013

ABSTRACT

Phalloidin, a toxin isolated from the death cap mushroom, *Amanita phalloides,* binds to filamentous actin with high affinity, and this has made fluorophore-conjugated phalloidin a useful tool in cellular imaging. Hepatocytes take up phalloidin via the liver-specific organic anion transporting polypeptide 1b2, but phalloidin does not permeate most living cells. Rapid entry of styryl dyes into live hair cells has been used to evaluate function, but the usefulness of those fluorescence dyes is limited by broad and fixed absorption spectra. Since phalloidin can be conjugated to fluorophores with various spectra, we investigated whether it would permeate living hair cells. When we incubated mouse utricles in 66 nM phalloidin-CF488A and followed that by washes in phalloidin-free medium, we observed that it entered a subset of hair cells and labeled entire hair bundles fluorescently after 20 min. Incubations of 90 min labeled nearly all the hair bundles. When phalloidin-treated utricles were cultured for 24 h after washout, the label disappeared from the hair cells and progressively but heterogeneously labeled filamentous actin in the supporting cells. We investigated how phalloidin may enter hair cells and found that P2 receptor antagonists, pyridoxalphosphate-6-azophenyl-2′, 4′-disulfonic acid and suramin, blocked phalloidin entry, while the P2Y receptor ligands, uridine-5'-diphosphate and uridine-5'-triphosphaste, stimulated uptake. Consistent with that, the P2Y6 receptor antagonist, MRS 2578, decreased phalloidin uptake. The results show that phalloidin permeates live hair cells through a pathway that requires metabotropic P2Y receptor signaling and suggest that phalloidin can be transferred from hair cells to supporting cells in culture.

Keywords: UDP, vestibular, balance, utricle, live cell imaging

INTRODUCTION

Styryl dyes, such as DASPEI, FM 1–43, and FM 4–64, can be used to label live hair cells (HC) in vitro and in vivo (Jorgensen 1989; Balak et al. 1990). Those dyes appear to rapidly enter hair cells through mechanotransduction channels that are in the open state and through ligand-gated P2X receptors (Gale et al. 2001; Meyers et al. 2003; Crumling et al. 2009). Yet, the broad and fixed absorption spectra of styryl dyes can be a hindrance for research that uses additional fluorescent probes. For example, FM 1–43 labeling could pose difficulties while using GFP-fluorescent tissue, since both FM 1–43 and GFP have similar absorbance spectra. For that reason, it would be advantageous to have other fluorophore choices to label live HCs.

Phalloidin, a toxin isolated from the mushroom, *Amanita phalloides,* binds to filamentous actin (F-actin) at the interface between subunits. Phalloidin has a high affinity for F-actin, and it lowers the critical actin concentration while increasing filament polymerization and stabilization (Dancker et al. 1975; Wieland et al. 1975; Faulstich et al. 1977; Estes et al. 1981; Coluccio and Tilney 1984).

Correspondence to: Jeffrey T. Corwin • Department of Neuroscience • University of Virginia School of Medicine • 409 Lane Rd, PO Box 801392, Charlottesville, VA 22908, USA. Telephone: +1-434-924-2524; Fax: +1-434-982-3966; email: corwin@virginia.edu

Fluorophore-conjugated phalloidin is widely used for visualizing F-actin in fixed, permeabilized tissue. Although phalloidin does not permeate most intact cell membranes, it permeates heptatocytes via liver-specific organic anion uptake transporting polypeptides (Frimmer et al. 1980; Walli et al. 1981; Faulstich et al. 1983; Munter et al. 1986; Petzinger and Frimmer 1988; Fehrenbach et al. 2003; Meier-Abt et al. 2004; Lu et al. 2008).

When low concentrations of fluorophore-conjugated phalloidin are microinjected into live cells it produces fiduciary marks that do not disrupt actin dynamics, allowing the microinjected phalloidin to be followed in vitro via fluorescent speckle microscopy. This provides dynamic measures of localized directions and rates of F-actin flow (Lin and Forscher 1995; Waterman-Storer et al. 1998; Schaefer et al. 2002, 2008; Burnette et al. 2008).

Here we report that fluorophore-conjugated phalloidin permeates live HCs in mouse utricles and that the fluorescence persists after aldehyde fixation. When phalloidin-treated utricles are cultured for 24 h after washout, the fluorescent label gradually disappears from HCs and appears in the neighboring supporting cells. Tests with pharmacological activators and inhibitors indicated that P2Y receptor signaling is required for the permeation of phalloidin into HCs and that uridine-5'-diphosphate (UDP) and uridine-5'-triphosphaste (UTP), which are agonists for a subset of P2Y receptors, enhance the permeation. We suspect that fluorophore-conjugated phalloidin might provide a tool useful for measuring the dynamics of actin assembly and turnover in the inner ear.

METHODS

Dissection of utricles

All animal experiments were performed according to protocols approved by the Animal Care and Use Committee at the University of Virginia. Swiss Webster mice were obtained from Charles River Labs (Wilmington, MA). Pups were anesthetized on ice and then decapitated. Adult mice were killed by CO_2 asphyxiation and then decapitated. Temporal bones were dissected in ice-cold Dulbecco's modified Eagle's medium (DMEM)/F-12 (Invitrogen, Carlsbad, CA), where the utricles were isolated, the roof dissected away, and the otoconia were removed using protease XXIV for 5 min (50 μg/mL, Sigma, St. Louis, MO).

Fluorophore-conjugated phalloidin treatment

The 2 μL of Cell Tak (BD Bioscience, San Jose, CA) was air-dried on 14 mm microwell glass-bottom culture dishes (MatTek, Ashland, MA). Live neonatal mouse utricles (P0 to P7) were plated nerve-side-down in 60 μl of DMEM/F-12 onto the dried Cell Tak. Phalloidin-CF488A (Biotium, Hayward, CA) was dissolved in water. After testing phalloidin-CF488A concentrations of 13.2 to 500 nM, we did not observe differences in uptake, and we used 66 nM phalloidin-CF488A for the analytical experiments reported here.

The 140 μl of DMEM/F-12 containing 94.29 nM phalloidin-CF488A and 1 % fetal bovine serum (FBS, Gibco) were added to the 60 μl volumes of culture media in the MatTek dishes to produce a final volume of 200 μl of 66 nM phalloidin-CF488A in each dish. Utricles were then incubated at 37 °C for 1 to 120 min, depending on the experiment. To wash out the phalloidin-containing media, 1 mL of DMEM/F-12 was added to each dish, and after 30 s, 1 mL was removed. This was repeated three times. For live imaging, utricles were gently lifted off the dish with fine forceps and mounted nerve-side-up in a 60 μl drop of DMEM/F-12 on a coverglass chamber. Coverglass chambers were prepared by adhering two strips of double-sided Scotch tape to create a bridge with the tape acting as spacers so that, when utricles were mounted between the top and bottom coverglasses, the hair bundles were not bent or damaged. The utricle remained in place for imaging after the smaller top coverglass was placed over it. All images of live utricles were taken within 10 min.

To examine whether unconjugated CF488A fluorophore alone would permeate into cells of the inner ear, live neonatal utricles were plated on air-dried Cell Tak in Mat Tek dishes in 60 μl of DMEM/F-12 as described above. CF488A, amine (Biotium, Hayward, CA) was dissolved in water. The 140 μl of DMEM/F-12 containing 94.29 nM CF488A and 1 % fetal bovine serum (FBS, Gibco) were added to the 60 μl volumes of culture medium in the MatTek dishes to produce a final volume of 200 μl of 66 nM CF488A in each dish. Utricles were then incubated at 37 °C for 30 min. The CF488A-containing media was then washed out as described above, and the utricles were then imaged live.

In some experiments, mounted utricles were treated with 66 nM Alexa Fluor 647 phalloidin for 20 min. The phalloidin-containing medium was then washed out three times with DMEM/F-12, and the utricles were exposed to 5 μM FM 1–43 in DMEM/F-12 for 10 s as previously described (Meyers et al. 2003). Then, that was washed out with three changes of DMEM/F-12, and the utricles were imaged live.

In other experiments, after the three washes in label-free medium, fresh DMEM/F-12 containing 1 % FBS, 0.25 μg/ml Fungizone, and 10 μg/ml ciprofloxacin (Bayer, Berlin, Germany) were added back to the dish, and the utricles were cultured in that phalloidin-free medium at 37 °C for either 3, 6, 12, 18, 24 h, or 7 days.

Aldehyde fixation and actin staining

For certain experiments, live phalloidin-treated utricles were washed three times with phalloidin-free DMEM/F-12 and fixed for 25 min in 4 % paraformaldehyde in phosphate-buffered saline (PBS) at room temperature (RT), then imaged directly or after staining in Alexa Fluor 647 phalloidin (132 nM) in PBS containing 0.2 % Triton X-100 (PBST). Samples were mounted in SlowFade (Invitrogen), and images were taken with Zeiss LSM 510 and Zeiss LSM 710 confocal microscopes. Images of control and drug-treated groups were acquired using identical exposure settings to allow for comparisons between the groups.

To compare fluorescence between utricles that were treated with phalloidin-CF488A before fixation and utricles treated with phalloidin-CF488A after fixation, freshly dissected neonatal utricles were separated into two groups. One group of utricles was treated live with 66 nM phalloidin-CF488A for 30 min as described above. These utricles were then fixed with 4 % paraformaldehyde for 25 min and imaged as described. The other group of freshly dissected utricles was treated with protease XXIV for 5 min (50 μg/mL, Sigma, St. Louis, MO) and then fixed with 4 % paraformaldehyde in PBS for 25 min. After the fix was washed out with three washes of PBS, the utricles were then incubated in 200 μl of 66 nM phalloidin-CF488A (dissolved in water) for 30 min at room temperature. Utricles were then washed with PBS and imaged.

Immunocytochemistry

Mouse anti-myosin VIIA (1:100, Developmental Studies Hybridoma Bank) and rabbit anti-Sox2 (1:1000, Millipore, Temecula, CA) were used to label hair cell somata and supporting cell nuclei, respectively. Fixed utricles were washed in PBS and then incubated for 30 min at RT with PBST and 10 % normal goat serum (Vector Laboratories, Burlingame, CA). Samples were then incubated overnight in primary antibodies in PBST with 2 % normal goat serum. The next day, samples were washed three times with PBS and then incubated with Alexa-conjugated secondary antibodies (1:200, Invitrogen) in PBST for 1 hr at RT. Then, utricles were rinsed in PBS three times and mounted in SlowFade for imaging.

Examination of phalloidin uptake using pharmacological antagonists

To investigate whether phalloidin permeation requires P2 receptor signaling, utricles were incubated in the P2 receptor antagonists pyridoxalphosphate-6-azophenyl-2′, 4′-disulfonic acid (PPADS, 100 μM, Tocris Biosciences, Ellisville, MO, for 15 min at 37 °C) or suramin (Sigma, 100 μM, for 15 min at 37 °C). In some experiments, utricles were pre-treated with PPADS (100 μM, 15 min at 37 °C), then incubated with PPADS (100 μM) and phalloidin-CF488A (66 nM) for 90 min at 37 °C. After three washes in DMEM/F-12, the utricles were incubated an additional 90 min at 37 °C with 66 nM phalloidin-CF488A to test whether the PPADS treatment would lead to a persistent inhibition of phalloidin permeation. After three additional washes in phalloidin-free DMEM/F-12, those utricles were imaged live. In other experiments, mounted utricles that had been treated with PPADS were exposed to PPADS and 5 μM FM 1–43 in DMEM/F-12 for 10 s as previously described (Meyers et al. 2003), then that was washed out with three changes of DMEM/F-12, and the utricles were imaged live.

To investigate P2 receptor agonists that might enhance permeation of phalloidin-CF488A, we incubated utricles with either adenosine 5'-triphosphate (ATP, 1 mM, Sigma), 2′(3′)-*O*-(4-Benzoylbenzoyl)adenosine-5′-triphosphate tri(triethylammonium) (BzATP, 100 μM, Tocris), adenosine 5'-diphosphate (ADP, 1 mM, Sigma), uridine 5'-triphosphate (UTP, 1 mM, Sigma), uridine 5'diphosphoglucose disodium (UDP-glucose, 1 mM, Sigma), or uridine 5'-diphosphate (UDP, 1 mM, Tocris) for 15 min at 37 °C. Then they were incubated an additional 20 min at 37 °C with both the respective nucleotide and phalloidin-CF488A (66 nM), and rinsed three times in DMEM/F-12 before they were imaged live or before fixation in 4 % paraformaldehyde.

To investigate whether phalloidin permeation requires P2Y6 receptors, we used MRS 2578, a potent antagonist for P2Y6 receptors. MRS 2578 was dissolved in dimethyl sulfoxide (DMSO) (Sigma). Utricles were treated with MRS 2578 for 15 min at 37 °C. Utricles were then cultured an additional 20 min at 37 °C with MRS 2578 and phalloidin-CF488A (66 nM). After three washes in DMEM/F-12, utricles were fixed with 4 % paraformaldehyde as above and imaged. MRS 2578-treated utricles were compared against vehicle controls.

To investigate whether phalloidin permeation requires PLC or PKC second messenger signaling, we used U-73122 hydrate (10 μM, Sigma), an inhibitor of phospholipase C, and bisindolylmaleimide II (BIM II; 50 μM, Sigma), an inhibitor of all protein kinase C subtypes. These drugs were dissolved in DMSO. Utricles were treated with individual drugs for 20 min at 37 °C. Utricles were then cultured an additional 20 min at 37 °C with the respective drug and phalloidin-CF488A (66 nM). After three washes in DMEM/F-12, utricles were fixed with 4 % paraformaldehyde as above and imaged. Fluorescence levels in U-73122- and BIM II-treated utricles

were compared against vehicle controls. Additionally, to investigate whether these pharmacological inhibitors would be sufficient to prevent agonist-induced stimulation of phalloidin-CF488A uptake, utricles were treated with 1 mM UDP and either U-73122 or BIM II for 20 min at 37 °C. They were then cultured an additional 20 min at 37 °C with UDP and the respective drug and phalloidin-CF488A (66 nM). After three washes in DMEM/F-12, utricles were fixed with 4 % paraformaldehyde as above and imaged. Fluorescence was compared against vehicle controls.

To test for an involvement of OATs or OATPs in the permeation of phalloidin, utricles were treated with probenecid (2 mM, Sigma). Utricles were treated with probenecid for 20 min at 37 °C. They were then cultured an additional 20 min at 37 °C with the probenecid and phalloidin-CF488A (66 nM). After three washes in DMEM/F-12, utricles were fixed with 4 % paraformaldehyde as above and imaged. Utricles were compared against vehicle controls.

To test for the involvement of pannexin channels in the permeation of phalloidin into hair cells, utricles were treated with 100 μM carbenoxolone (CBX, Sigma) for 15 min at 37 °C. Utricles were then cultured an additional 20 min at 37 °C with the drug and phalloidin-CF488A (66 nM). After three washes in DMEM/F-12, utricles were fixed with paraformaldehyde and imaged.

RNA extraction, RT-PCR, and quantitative PCR

To delaminate the sensory epithelium, utricles from P5 mice were incubated in thermolysin (0.5 mg/ml in DMEM/F-12; Sigma) at 37 °C for 60 minutes, and then transferred to DMEM/F-12 where the macula and its surrounding non-sensory epithelium were carefully separated from the underlying stromal tissue in each utricle by microdissection (Saffer et al. 1996). Delaminated epithelia and stromal tissue samples were collected and pooled separately. RNA was extracted from those samples as well as from P0 kidney and liver tissue using the RNAqueous kit (Ambion) according to the manufacturer's protocol. Poly-A RNA was reverse transcribed using a High Capacity RNA-to-cDNA kit (Applied Biosystems) and quantitative PCR was performed in triplicate (i.e., starting material was collected and pooled three times independently) using a SensiMix SYBR Green and Fluorescein kit (Quantace) on a MyIQ/iCycler (Biorad). *Cyclophilin* was used as an endogenous reference. Gene expression was analyzed using the Real-time PCR miner algorithm (Zhao and Fernald 2005). The following primers were used: *Cyclophilin* (Forward: CAGTGCTCAGAGCTCGAAAGT; Reverse: GTGTTCTTCGACATCACGGC), *Oat1* (Forward: TGCACAGTTGGCCTCCCTGC; Reverse: GCTCACTATGCTGCCCACCCG), *Oatp2b1* (Forward: AGCAGGGCTTCTACCACACCTGA; Reverse: TCCTGTCTGGCATCCGGGGC), *Oatp3a1* (Forward: AAACCACGAGGGCGGGCTGA; Reverse: GCAGCCCTCAGCTTCGCACAA), *Oatp1b2* (Forward: TCGCCAGCCTAGGCCAAATGC; Reverse: TGGGCAGCTTTGCTTGGATGCT), and *Oatp2a1* (Forward: GGGACGGTGCCCATTCAGCC; Reverse: GGCTCCGATCCACCGAGGGT).

For RT-PCR analysis, cDNA was prepared as described above from 100 ng total RNA extracted from the delaminated P5 mouse utricle sensory epithelium and stroma samples. Control experiments testing for the presence of genomic DNA contamination in the RNA where no reverse transcriptase was added to the reactions were negative (data not shown). mRNA expression was evaluated on a MyIQ/iCycler (Biorad) using *Taq* DNA Polymerase (1 unit final, Invitrogen), 10X PCR Buffer (Invitrogen), 2 mM $MgCl_2$ (Invitrogen), and 0.2 mM dNTP mix (Invitrogen).

The following PCR primers were used: *Cyclophilin* (Forward: CAGTGCTCAGAGCTCGAAAGT; Reverse: GTGTTCTTCGACATCACGGC), *P2Y1* (Forward: AGGAAAGCTTCCAGGAGGAG; Reverse: CGTGTCTCCATTCTGCTTGA), *P2Y2* (Forward: GTCAGCAGTGACGACTCAAGAC; Reverse: TCAGAGGATATCAGCCCCTTTA), *P2Y4* (Forward: GCAGGCGTGAAGTGAGGCCA; Reverse: TGGAGGGTAAGGAGCACCATCTTAG), *P2Y6* (Forward: GGCGGCTCGTATGGCTGTGG; Reverse: GCAAGAGACACCGGGCGTGG), *P2Y12* (Forward: CCGCACGGACACTTTCCCGTA; Reverse: TGCCGGTGAAGGTGAGTTGCC), *P2Y13* (Forward: GGCCACTAGATGTCACCTTTTC; Reverse: GATGGTGGGGTGGTAACTAGAA), *P2Y14* (Forward: GGAATTCTCTCTTCCGAATCCT; Reverse: TGTTCATCTTCTCACCTCTGGA). Primers were first tested using cDNA synthesized from RNA extracted from P5 mouse brain.

Specimens were preheated at 94 °C for 3 min followed by 35 cycles at 94 °C for 30 sec, 60 °C for 30 sec, and 72 °C for 30 sec, then 72 °C for 2 min. PCR products were then separated on a 1 % agarose gel.

Data analysis

Each experiment was repeated at least three times and analyzed with Student's *t*-test or one-way ANOVA with Newman-Keuls Multiple Comparisons post-test (GraphPad Prism; α level=0.05 in all cases). All descriptive statistics are presented as the mean± S.E.M. All Student's *t*-test analyses were performed with two-tails. Images were carefully selected to demonstrate the average effect.

RESULTS

Phalloidin permeates live hair cells and supporting cells in mouse utricles

To determine whether phalloidin could permeate and fluorescently label cells in living mouse utricles, we bathed utricles in phalloidin-CF488A for 20 min. We counted the number of hair cells and supporting cells phalloidin-CF488A permeated into. We identified HCs based upon the presence of fluorescent hair bundles or cuticular plates and we identified supporting cells based upon an absence of a hair bundle and cuticular plate and the presence of their characteristic circumferential F-actin belts, which are shown in the inset in Figure 1B. In each utricle, we detected 83.0±11.8 fluorescent hair bundles and 37.8±5.9 fluorescent supporting cells (Fig. 1A, B; n=24). We also detected punctate fluorescence throughout the sensory epithelium. These results indicate that phalloidin-CF488A can permeate both hair cells and supporting cells.

We tested whether phalloidin-CF488A could permeate into auditory HCs by incubating neonatal mouse cochleae in phalloidin-CF488A for 20 min as described (n=6). When we imaged these live cochleae we observed that many of the HCs had become highly fluorescent. Thus, the permeation of phalloidin-CF488A is not limited to vestibular HCs (Fig. 1C).

We incubated utricles for 90 min to determine whether longer incubations would allow more cells to take up the phalloidin. Phalloidin permeated more hair cells and supporting cells, as we observed 906± 74.6 fluorescent hair bundles (Student's $t$test, $t(27)$= 20.04, p<0.0001, Fig. 1D, E; n=5) and 225±72.1 fluorescent supporting cells (Student's $t$test, $t(27)$= 5.641, p<0.0001, Fig. 1D, E; n=5). This indicates that phalloidin can permeate living hair cells and supporting cells, but the permeation is not rapid.

To ensure that this labeling phenomenon was not due to any unique properties of the CF488A fluorophore, we also incubated utricles with phalloidin conjugated to Texas Red, Alexa Fluor 488, Alexa Fluor 568, and Alexa Fluor 647. In each of these experiments we observed comparable labeling patterns (data not shown). We also incubated utricles with unconjugated CF488A fluorophore. After we bathed utricles for 30 min with 66 nM CF488A, we did not detect any fluorescence (Fig. 1F). This suggests that the fluorophore-conjugated phalloidin entry into hair cells and supporting cells is due to the unique properties of phalloidin.

We investigated whether phalloidin-CF488A permeation impairs the capacity for hair cells to take up a brief exposure (10 sec) of FM 1–43. Rapid uptake of FM 1–43 is considered an indicator of functional mechanotransduction channels (Meyers et al. 2003). For this, we incubated utricles for 20 min with phalloidin conjugated to Alexa Fluor 647. After washing out the Alexa Fluor 647 phalloidin, we incubated the utricles for 10 sec with FM 1–43. The FM 1–43 dye was then washed out and the utricles were imaged live. We detected both Alexa Fluor 647 phalloidin and FM 1–43 fluorescence in these utricles (Fig. 1G). HCs throughout the maculae took up FM 1–43, and the FM 1–43 labeling pattern in the HCs that were Alexa Fluor 647 phalloidin-positive appeared to be indistinguishable from that in the HCs that were Alexa Fluor 647 phalloidin-negative. The results suggest that the permeation of phalloidin-CF488A into HCs does not cause an overwhelming block of mechanotransduction channels.

Since phalloidin has a high affinity for F-actin, we tested whether it would remain bound in culture. We incubated utricles for 90 min with phalloidin-CF488A and then maintained them in phalloidin-free media for 24 hr. We found that the number of fluorescent hair bundles diminished, and supporting cells throughout the maculae became fluorescent (Fig. 1H, I; n=6).

We sought to determine more precisely when the label disappeared from hair cells and began to appear more robustly amongst supporting cells, so we fixed utricles at various time points after the phalloidin-CF488A incubation (Fig. 2). Hair bundles were fluorescent 3 hr after the phalloidin washout. However, by 12 hr there were noticeable gaps in fluorescence throughout the sensory epithelium. We detected only 298.3±64.7 fluorescent hair bundles at this time, significantly less than after the 0 hr timepoint (Student's $t$test, $t(9)$=6.183, p<0.0001, Fig. 2 B, H; n=6)., By 18 hr, supporting cells throughout the sensory epithelium had taken up the label and were fluorescent. These results show that after incubating utricles with phalloidin-CF488A, less than half the hair cells retain the label 12 hr after a washout and that nearly all the supporting cells take up the label and become fluorescent by 18 hr.

The absence of fluorescent labeling of HCs in phalloidin-CF488A treated utricles that were maintained in culture over extended periods of time (> 18 hr) led us to investigate whether HCs died or experienced deleterious effects after phalloidin-treated utricles were maintained in culture. To test for this, we treated P2 utricles with 66 nM phalloidin-CF488A as above, washed out the label, and then maintained the utricles in culture for 24 hr. At this time point, we fixed the utricles, immunolabeled them with a monoclonal antibody directed against myosin VIIA, which labels HCs, and then took high magnification confocal micrographs. We measured the density of myosin VIIA-positive HCs remaining in these cultures from 15 separate 50 μm x 50 μm regions from each cultured utricle. In utricles treated with phalloidin-CF488A, we detected an average HC density of 43.82 HCs/ 2500 μm^2 (n=3). This is comparable to the previously

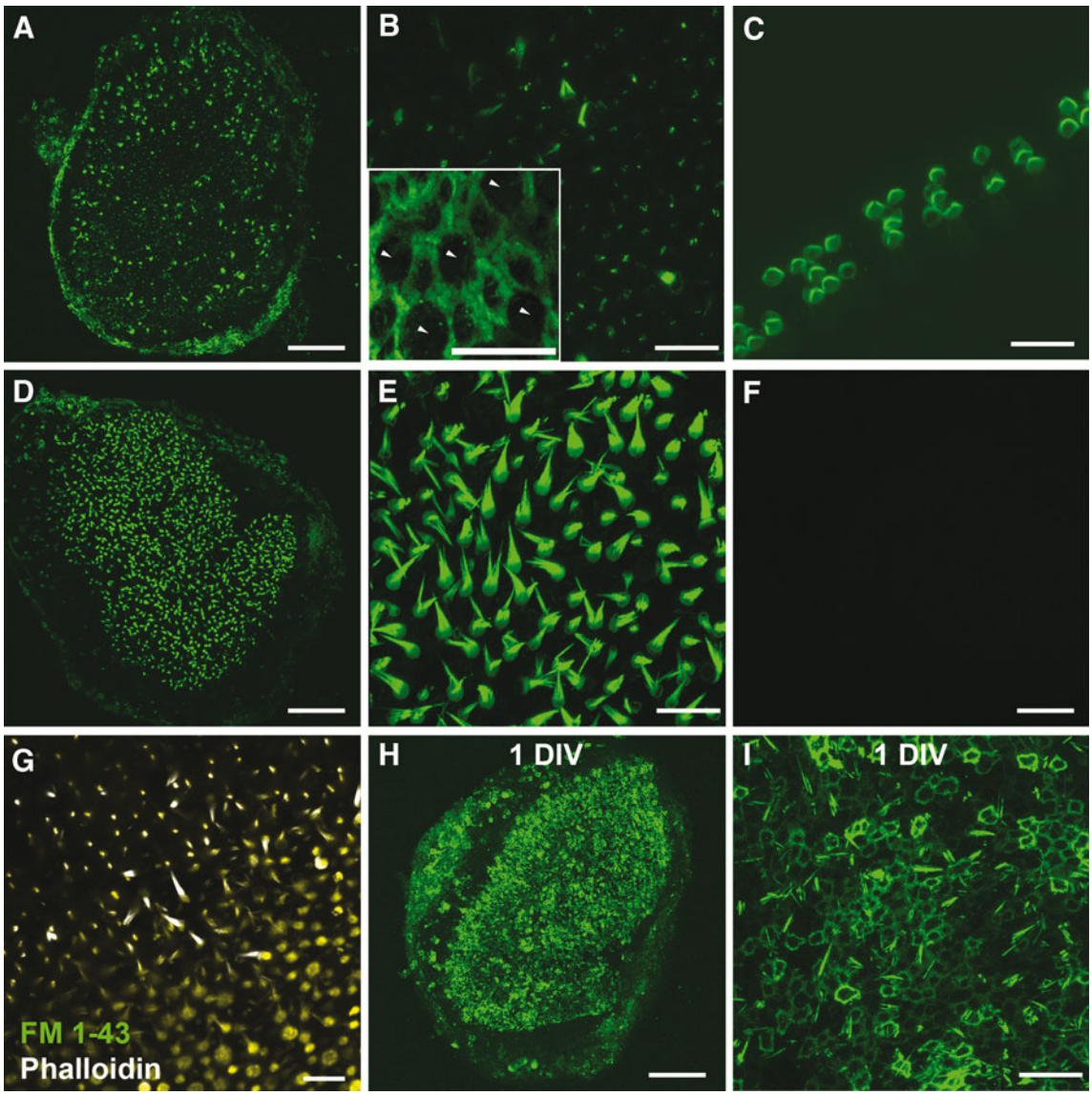

FIG. 1. Phalloidin permeates into live cells of the inner ear. **A** Maximum intensity Z-projection image of fluorescence observed after freshly dissected whole mount mouse utricles treated with phalloidin-CF488A for 20 min (37 °C) were imaged live. **B** Higher magnification from **(A)**. Fluorescence can be observed throughout the entire hair bundle in only a few hair cells and in a discrete, punctate location within the stereocilia in the majority of hair cells. *Inset* depicts characteristic circumferential F-actin belts found among supporting cells (P86 utricle). Five presumptive HCs, which characteristically have circular apical surfaces, have been labeled with *arrowheads* while the remaining cells display the thick circumferential F-actin belts characteristic of mouse utricle supporting cells. **C** Maximum intensity Z-projection image of fluorescence observed after whole mount mouse cochlea treated with phalloidin-CF488A for 20 min and imaged live. **D** Example image from a live utricle treated with phalloidin-CF488A for 90 min. **E** Higher magnification from **(D)** depicts phalloidin uptake throughout the entire hair bundle in nearly all hair cells with this longer treatment of phalloidin. **F** No fluorescence observed in mouse utricles treated with the CF488A fluorophore alone. **G** Hair cells are able to take up FM 1–43 after Alexa Fluor 647 phalloidin treatment. Mouse utricles were incubated with Alexa Fluor 647 phalloidin for 20 min. The Alexa Fluor 647 phalloidin was then washed out with DMEM/F-12. Utricles were then treated with FM 1–43 for 10 s. FM 1–43 was washed out, and the utricles were imaged live. **H, I** Fluorescence observed in the circumferential F-actin belts of supporting cells and a few stereocilia after utricles were maintained 1 DIV (24 h) after a phalloidin treatment. **I** High magnification region from **(H)**. Scale *bars* in **A**, **D**, **F,** and **H** are 100 μm; **B**, **C**, **E**, **G**, **I** are 20 μm; *inset* in **B** is 10 μm.

reported density of 46.75 HCs/2500 μm^2 in P2 mouse utricles that were fixed *in vivo* (Burns et al. 2012). Furthermore, P2 utricles maintained 24 hr in culture that were not treated with phalloidin-CF488A had 42.51 HCs/2500 μm^2 (Fig. 3). These results show that at least over the period of 24 hr, there is not a

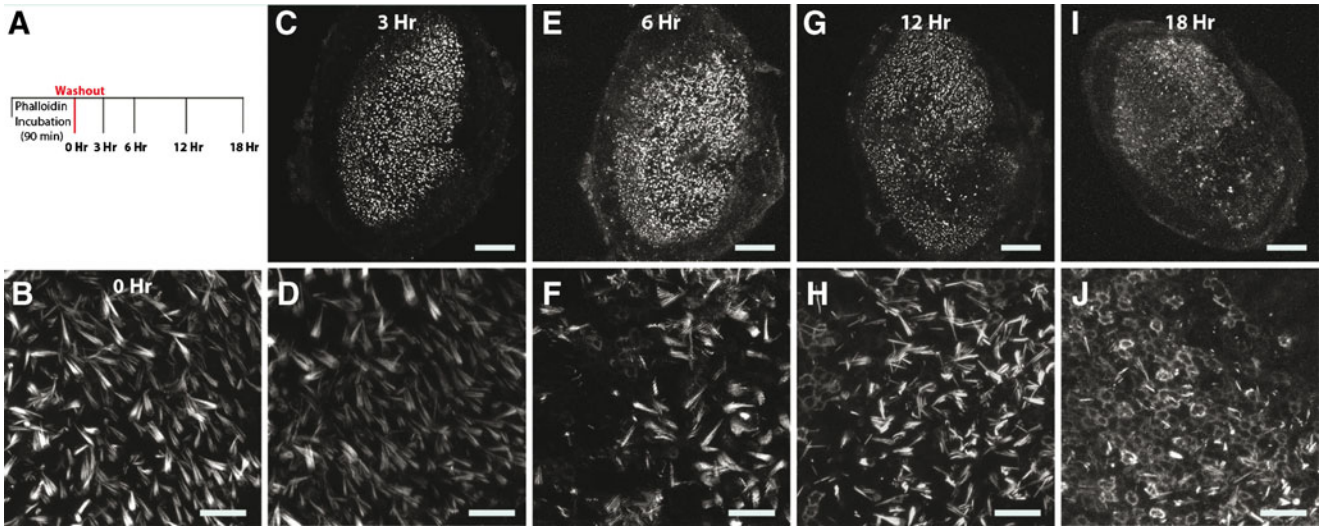

FIG. 2. Time series of fluorescence observed after culturing utricles that had been treated with phalloidin-CF488A. Fluorescence disappears from hair cells and appears within circumferential F-actin belts of supporting cells in culture. **A** Experimental outline. Utricles were treated with phalloidin-CF488A for 90 min, then the label was washed out three times with DMEM/F-12, and then the media was replaced with DMEM/F-12 containing 1 % FBS. Utricles were then maintained in culture at 37 °C. Utricles were mounted and imaged live immediately (0 h; **B**), or after 3 h **(C, D)**, 6 h **(E, F)**, 12 h **(G, H)**, or 18 h in culture **(I, J)**. Around 6 h, the label begins to disappear from hair cells and supporting cells become fluorescent **(F)**, and by 18 h, nearly all supporting cells are fluorescent **(J)**. Scale *bars* in **B**, **C**, **E**, **G**, and **I** are 100 μm; scale *bars* in **D**, **F**, **H**, and **J** are 20 μm.

substantial amount of HC degeneration resulting from the phalloidin-CF488A treatments.

We next sought to determine whether HCs in phalloidin-treated utricles maintain their hair bundles over longer periods in culture. For this, we treated four utricles with phalloidin-CF488A as described, washed out the phalloidin-containing medium, and then incubated the utricles in phalloidin-free culture medium for 7 days. After that, we fixed and permeabilized the utricles and incubated them with Alexa Fluor 647 phalloidin to stain all the F-actin. The presence of substantial numbers of Alexa Fluor 647 phalloidin labeled hair bundles in these utricles showed that the loss of phalloidin-CF488A fluorescence had not resulted from a substantial HC or hair bundle loss caused by the prior live treatment with phalloidin-CF488A and that the prior treatment did not cause substantial hair bundle losses even after long periods in culture (Fig. 3I–L).

The manner and the mechanism by which the label disappears from the hair bundles over time in culture remains unknown. However, we investigated whether HCs in cultured, phalloidin-treated utricles remained capable of taking up fluorophore-conjugated phalloidin. For this, we treated utricles with phalloidin-CF488A for 90 min, washed out the label, and then cultured them for 24 hr. After imaging two of these utricles, we confirmed that fluorescence was lost from the HCs at this time. The remaining utricles were then incubated with Alexa Fluor 647 phalloidin and imaged. We detected Alexa Fluor 647 phalloidin positive hair bundles throughout these utricles, suggesting that HCs in these cultured utricles remain capable of taking up fluorophore-conjugated phalloidin (data not shown, n=4).

We tested whether the fluorescent labeling pattern would change after fixation. We incubated utricles with phalloidin-CF488A for 20 min then fixed with paraformaldehyde. There were 84.33± 15.0 fluorescent hair bundles after fixation, which did not differ from what we observed in living utricles (Student's t-test, $t(28)=0.055$, $p=0.957$, Fig. 4A; n=6). From this we determined that the phalloidin-labeling pattern in hair cells is not changed with aldehyde fixation.

For deeper antibody penetration, many immunofluorescence protocols require detergents, such as Triton X-100, to permeabilize the tissue. We sought to determine whether using this detergent could alter the distribution of phalloidin labeling. We incubated fixed phalloidin-treated utricles in PBS containing 0.2 % Triton X-100 and 132 nM Alexa Fluor 647 phalloidin for 30 min at RT. We found that the fluorescence from the CF488A fluorophore, which is conjugated to the phalloidin used to treat the live utricles, became diffuse throughout the tissue (Fig. 4B). All F-actin structures throughout the epithelium displayed fluorescence with noticeable intensity differences. So while treating live utricles with fluorophore-conjugated phalloidin may produce a labeling pattern that persists after aldehyde

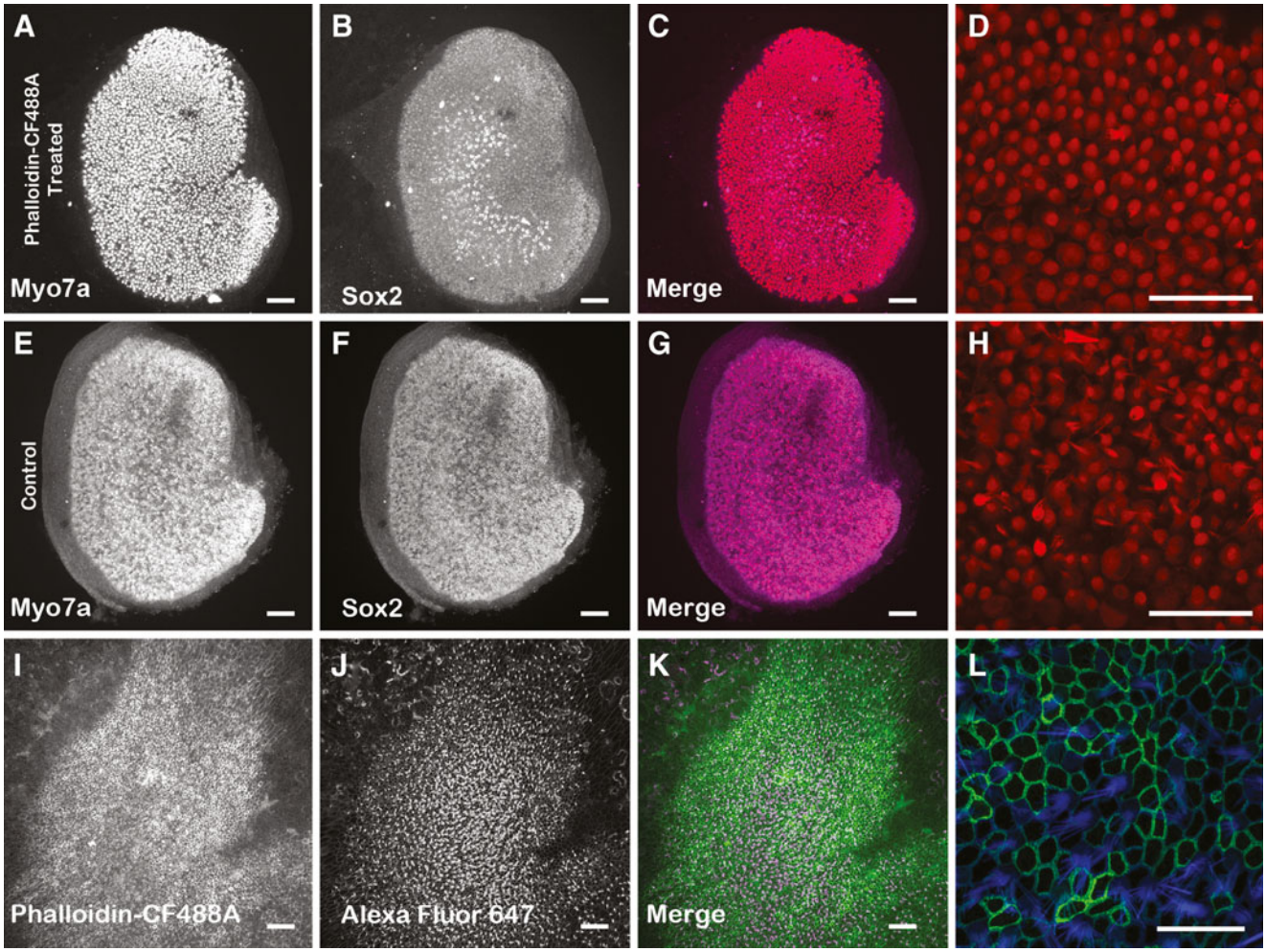

FIG. 3. Hair cell density was not affected in phalloidin-treated utricles maintained in culture 24 h. P2 mouse utricles were treated 90 min with 66 nM phalloidin-CF488A **(A–D)** and then maintained in culture for 24 h. The resulting hair cell density was compared against control P2 utricles that were maintained in culture for 24 h but were not treated with phalloidin-CF488A **(E–H).** After culturing, utricles were immunolabeled with myosin VIIa **(A, E)** and Sox2 **(B, F)**. The *merged ima*ges are also displayed in **C, G.** Higher magnification images of myosin VIIA immunofluorescence from utricles that were treated with phalloidin-CF488A **(D)** and utricles that were not phalloidin-treated **(H)**. There were no differences in HC density per 2,500 μm^2 in these utricles. **I–L** Maximum intensity Z-projection images of utricles that were treated live with phalloidin-CF488A, then maintained in culture for 7 days, fixed, and additionally stained with Alexa Fluor 647 phalloidin. **I** Utricles that were treated with phalloidin-CF488A maintained the fluorescence after 7 days in culture. **J** Staining with Alexa Fluor 647 phalloidin reveals that these utricles still have HCs. **K** Merge. **L** Higher magnification of region showing fluorescence from phalloidin-CF488A (*green*) and Alexa Fluor 647 phalloidin. Scale *bars* in **A–C**, **E–G**, and **I–K** are 100 μm; scale *bars* in **D**, **H** are 50 μm; scale *bar* in **L** is 20 μm.

fixation, treatment with detergents such as Triton-X 100 can cause the fluorescence to become diffuse.

We investigated whether the permeation of phalloidin-CF488A into cells of the inner ear involves an active pathway (channel), or whether it would also be able to permeate into fixed tissues. For this, we compared fluorescence between utricles that were treated with phalloidin-CF488A before fixation to utricles that were treated with phalloidin-CF488A after fixation (Fig. 5). Utricles were incubated with 66 nM phalloidin-CF488A for 20 min, washed three times, fixed with 4 % paraformaldehyde and then imaged (Fig. 5C). Fluorescence in these were compared against utricles that were dissected, fixed with 4 % paraformaldehyde, then treated with 66 nM phalloidin-CF488A for 20 min (Fig. 5D). To compare uptake amongst samples, we measured average fluorescence intensities in five 100 μm x 100 μm regions of the sensory epithelium from maximum projection images using ImageJ (NIH) (Fig. 5A). We normalized fluorescent intensities to the mean intensities in controls. We detected significantly more fluorescence in the utricles treated with phalloidin-CF488A before fixation (Student's *t*-test, $t(4)=4.173$, $p=0.014$, Fig. 5B). This suggests that the permeation of phalloidin-CF488A into sensory cells of the utricle involves an active pathway.

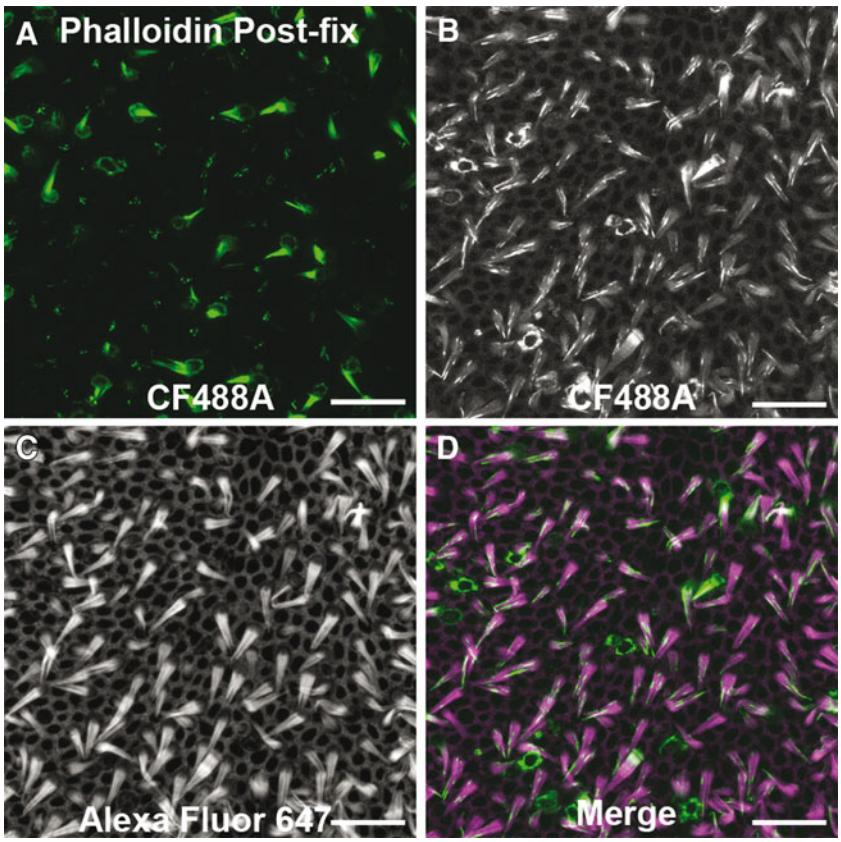

FIG. 4. Phalloidin permeation in live cells of inner ear is fixable. Example image of a utricle treated live with phalloidin-CF488A for 30 min then fixed with 4 % paraformaldehyde **(A). B–D** CF488A fluorescence maintained after phalloidin-CF488A-treated utricles were fixed as in **(A)**, and then counterstained with Alexa Fluor 647 phalloidin. Permeabilizing the post-fixed tissue to stain with Alexa Fluor 647 phalloidin causes the CF488A fluorescence to become more diffuse. Scale *bars* in **A–D** are 20 μm.

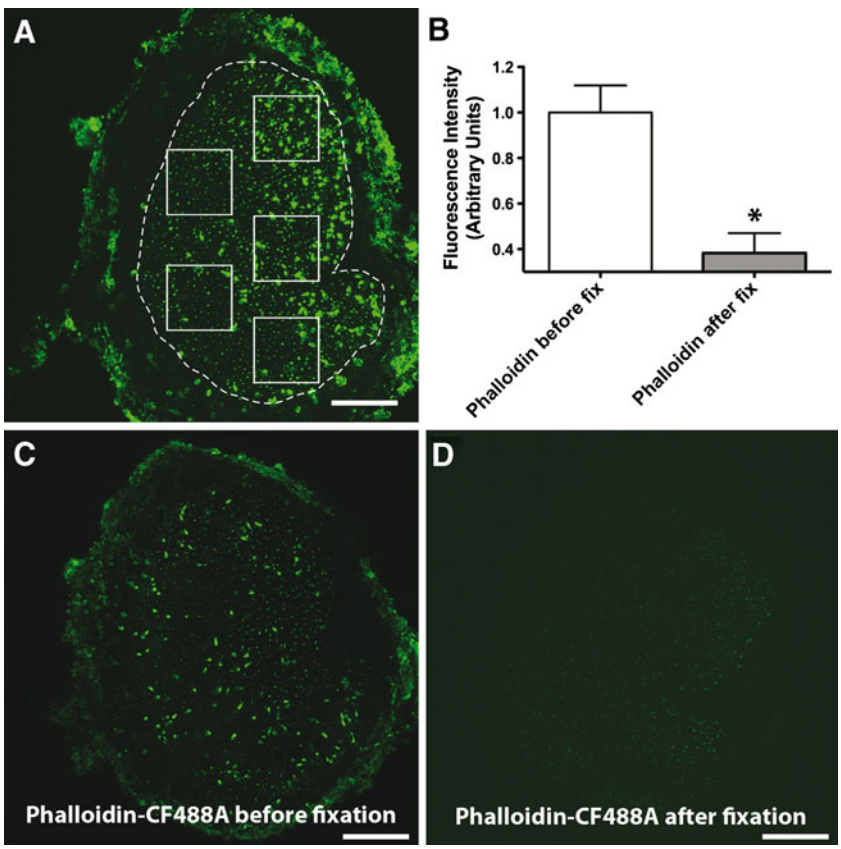

FIG. 5. Phalloidin permeation into live cells of inner ear involves an active pathway. **A** Mean fluorescence intensity was measured in five separate 100× 100 μm regions as depicted in the example image. **B** We observed more fluorescence in utricles that were treated with phalloidin-CF488A before fixation compared with utricles treated with phalloidin-CF488A after fixation (Student's *t*test, p=0.014). **C** Example micrograph of utricle treated with 66 nM phalloidin-CF488A and then fixed. **D** Example confocal micrograph of utricle fixed with paraformaldehyde for 20 min then treated with 66 nM phalloidin-CF488A. Scale *bars* are 100 μm.

P2 receptors contribute to the permeation of phalloidin into hair cells

P2 receptors are involved in the permeation of large molecular weight molecules and dyes including YO-PRO-1, TO-PRO-1, ethidium, lucifer yellow, and calcein (Surprenant et al. 1996; North 2002; Cankurtaran-Sayar et al. 2009). P2 receptors are subdivided into two distinct families: P2X and P2Y receptors. P2X receptors have two plasma membrane-spanning domains and respond to extracellular ATP as gated, cation-selective channels. In contrast, P2Y receptors are metabotropic, G protein-coupled receptors (GPCR) with seven transmembrane domains, and various P2Y family members have shown coupling to $G_{q/11}$, G_i, or G_s proteins (Housley 1998; Housley et al. 2009; Housley and Gale 2010).

HCs express both P2X and P2Y receptors (Housley et al. 1992; Housley et al. 1998; Housley et al. 1999; Szücs et al. 2004; Huang et al. 2010). We investigated whether these receptors are required for phalloidin entry through hair cells using PPADs and suramin, non-selective P2 antagonists (Lambrecht et al. 1992; Li 2000; Surprenant et al. 2000; Lambrecht et al. 2002; North 2002; Trujillo et al. 2006). We pre-incubated utricles with the antagonist for 15 min, then applied phalloidin-CF488A in the presence of the antagonist for 90 min. We found that both PPADS and suramin effectively blocked phalloidin uptake. Phalloidin only permeated into 4.3±1.2 hair cells in the presence of PPADS, a significant decrease compared to controls (Student's *t*-test, $t(30)=3.801$, $p=0.0007$, Fig. 6B; $n=8$). Suramin similarly decreased phalloidin uptake, where only 15.3±11.6 hair cells were fluorescent (Student's *t*-test, $t(26)=2.278$, $p=0.0312$, Fig. 6E; $n=4$). We fixed PPADS- and suramin-treated utricles and stained them with Alexa Fluor 647 phalloidin to confirm that hair cells were still present (Fig. 6C, D). These results indicate that P2 receptor signaling is required for phalloidin entry into live hair cells.

The styryl dye FM 1–43 enters mechanotransduction channels that are in the open state (Meyers et al. 2003). FM 1–43 is also widely used to investigate whether hair cells possess functional mechanotransduction currents (Kawashima et al. 2011). We applied FM 1–43 to PPADS-treated utricles to determine whether PPADS interferes with mechanotransduction, and found that these hair cells had normal FM 1–43 uptake (Fig. 6F; $n=4$). These results are consistent with the hypothesis that the decreased dye uptake is not due to an effect of PPADS on the mechanotransduction channel.

The inhibition of P2 receptor signaling by PPADS is reversible (Li 2000). Accordingly, we found that while uptake of phalloidin-CF488A was blocked in the presence of PPADS (Fig. 6G), hair cells were able to take up phalloidin-CF488A after PPADS was washed out (Fig. 6H). This indicates that the PPADS-mediated inhibition of phalloidin permeation is reversible.

P2Y nucleotide agonists enhance phalloidin-CF488A permeation

P2X and P2Y receptors are extracellularly gated by purine and pyrmidine nucleotides. In pharmacological studies, ATP is a major agonist for all P2X receptors and BzATP can potently activate P2X7 receptors. ADP, UTP, UDP, and UDP-glucose are major agonists that activate specific P2Y receptor subtypes (North 2002). We individually pretreated utricles with these to determine which P2 receptor subtypes might be involved in the phalloidin permeation.

We found that ATP decreased phalloidin uptake by 32.3 % (One-way analysis of variance [ANOVA] with Newman-Keuls Multiple Comparisons test, $p<0.05$, Fig. 7A, C; $n=12$). While extracellular ATP activates P2X channels, it can antagonize P2Y receptor subtypes (Kennedy et al. 2000). We observed no significant differences in fluorescence in utricles pretreated with BzATP, another P2X agonist (One-way ANOVA with Newman-Keuls Multiple Comparisons test, $p>0.05$, Fig. 7A, D; $n=9$). This indicates that P2X channels are not required for phalloidin uptake.

We further examined fluorescence from phalloidin-CF488A permeation upon pretreating with P2Y agonists. ADP, an agonist for P2Y1, P2Y12, and P2Y13 receptors, did not increase fluorescence from phalloidin-CF488A labeling (One-way ANOVA with Newman-Keuls Multiple Comparisons test, $p>0.05$, Fig. 7A, E; $n=6$). We also observed no significant differences in fluorescence after treating with UDP-glucose, a P2Y14 agonist (One-way ANOVA with Newman-Keuls Multiple Comparisons test, $p>0.05$, Fig. 7A, G; $n=4$). However, UTP (P2Y2, P2Y4, and P2Y6), increased fluorescence by 29 % (One-way ANOVA with Newman-Keuls Multiple Comparisons test, $p<0.05$, Fig. 7A, F; $n=11$). Another P2Y agonist, UDP (P2Y6), enhanced fluorescence by 56 % (One-way ANOVA with Newman-Keuls Multiple Comparisons test, $p<0.05$, Fig. 7A, G; $n=6$). These results implicate P2Y receptor signaling in the uptake of phalloidin.

P2Y-PLC-PKC signaling contributes to the permeation of fluorophore-conjugated phalloidin

We evaluated the presence of P2Y receptor subtype expression in the neonatal utricular maculae and underlying stroma using RT-PCR (Fig. 8A; $n=3$). We detected mRNA expression of P2Y1, P2Y2, P2Y6, P2Y13, and P2Y14 in the maculae. Since P2Y6 can be activated by both UTP and UDP, we evaluated the effects of MRS 2578, a P2Y6

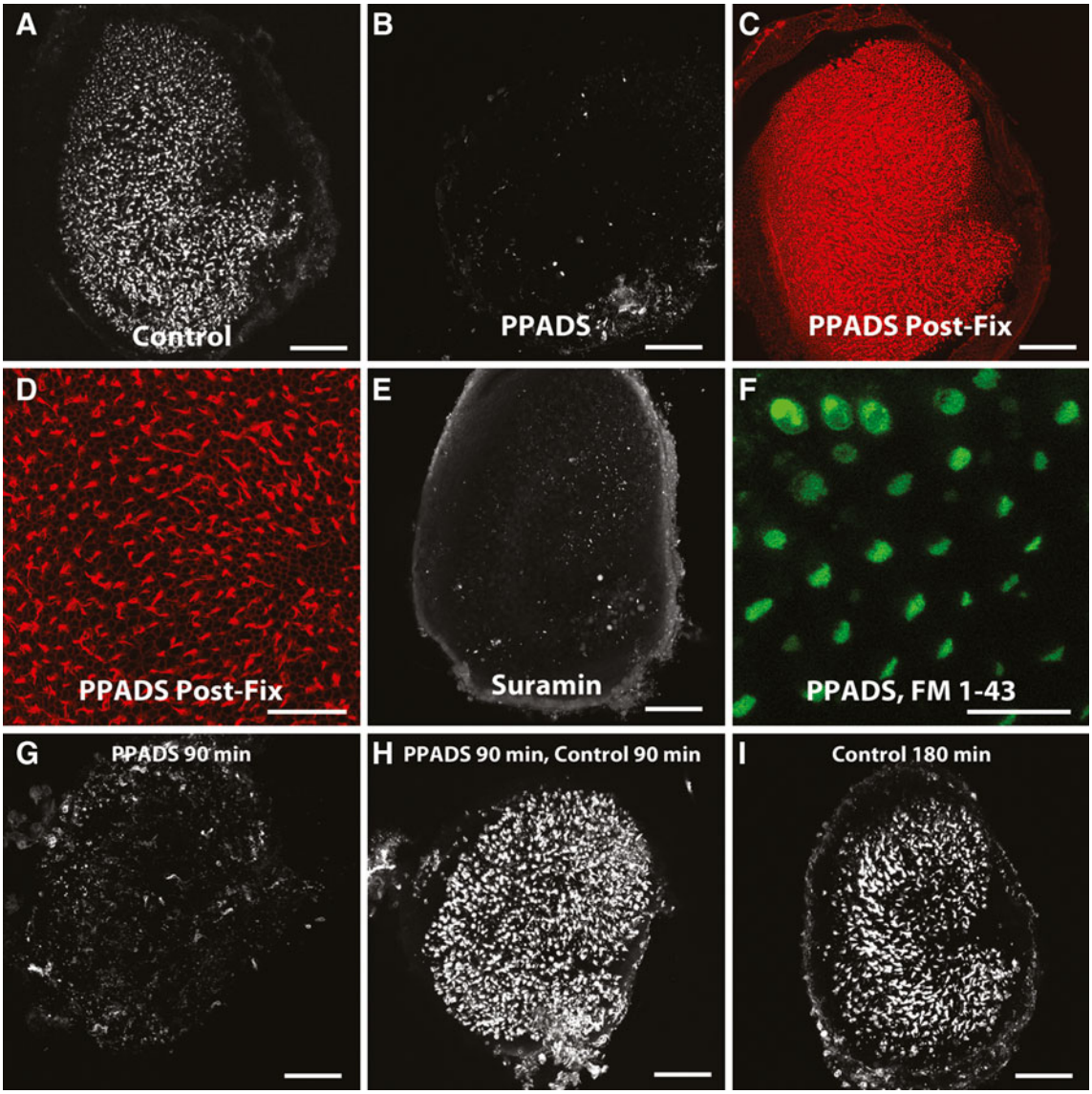

FIG. 6. Effects of P2 receptor blockers on fluorophore-conjugated phalloidin permeation. Blockers of P2 receptors inhibit phalloidin uptake. **A** Example image of a control living utricle treated with phalloidin-CF488a as described. **B** Example image of a living utricle treated with P2 antagonist PPADS (100 µm, *n*=8) and then incubated with PPADS and phalloidin-CF488A. Living PPADS-treated utricle from **(B)** was fixed and counterstained with phalloidin-Alexa Fluor 568 to visualize the entire F-Actin network and ensure that hair cells were still present **(C, D). E** Example image of a living utricle treated with P2 antagonist suramin (100 µm, *n*=4). **F** PPADS-treated living utricle was co-incubated for 10 s with PPADS and 5 µM FM 1-43 and then imaged showing that PPADS does not inhibit mechanotransduction. **G–I** Washing out PPADS restores the ability of hair cells to take up phalloidin-CF488A. **G** Example image of a utricle treated with 100 µm PPADS for 90 min at 37 °C. **H** After PPADS treatment and several washes in DMEM/F-12, some utricles were maintained in 66 nM phalloidin-CF488A for 90 min at 37 °C and imaged live. Phalloidin was able to enter the hair cells in these utricles at levels comparable to control utricles treated 180 min in 66 nM phalloidin-CF488A at 37 °C **(I).** Scale *bars* in **A–C**, **E**, and **G–I** are 100 µm; scale *bar* in **D**, and **F** are 50 µm.

antagonist, on the permeation of phalloidin-CF488A (Mamedova et al. 2004). Treating with 500 nM MRS 2578 decreased the resulting fluorescence by 27.0 % (Student's *t*-test, $t(16)=3.498$, $p=0.003$, Fig. 8B; $n=4$). This is consistent with the hypothesis that P2Y6 signaling is involved in the permeation of phalloidin. While PPADs and suramin almost completely prevented the permeation of phalloidin-CF488A into hair cells, MRS 2578 significantly decreased fluorescence by only 27.0 %. We tested MRS 2578 at 500 nM, a concentration higher than the IC_{50} of 98

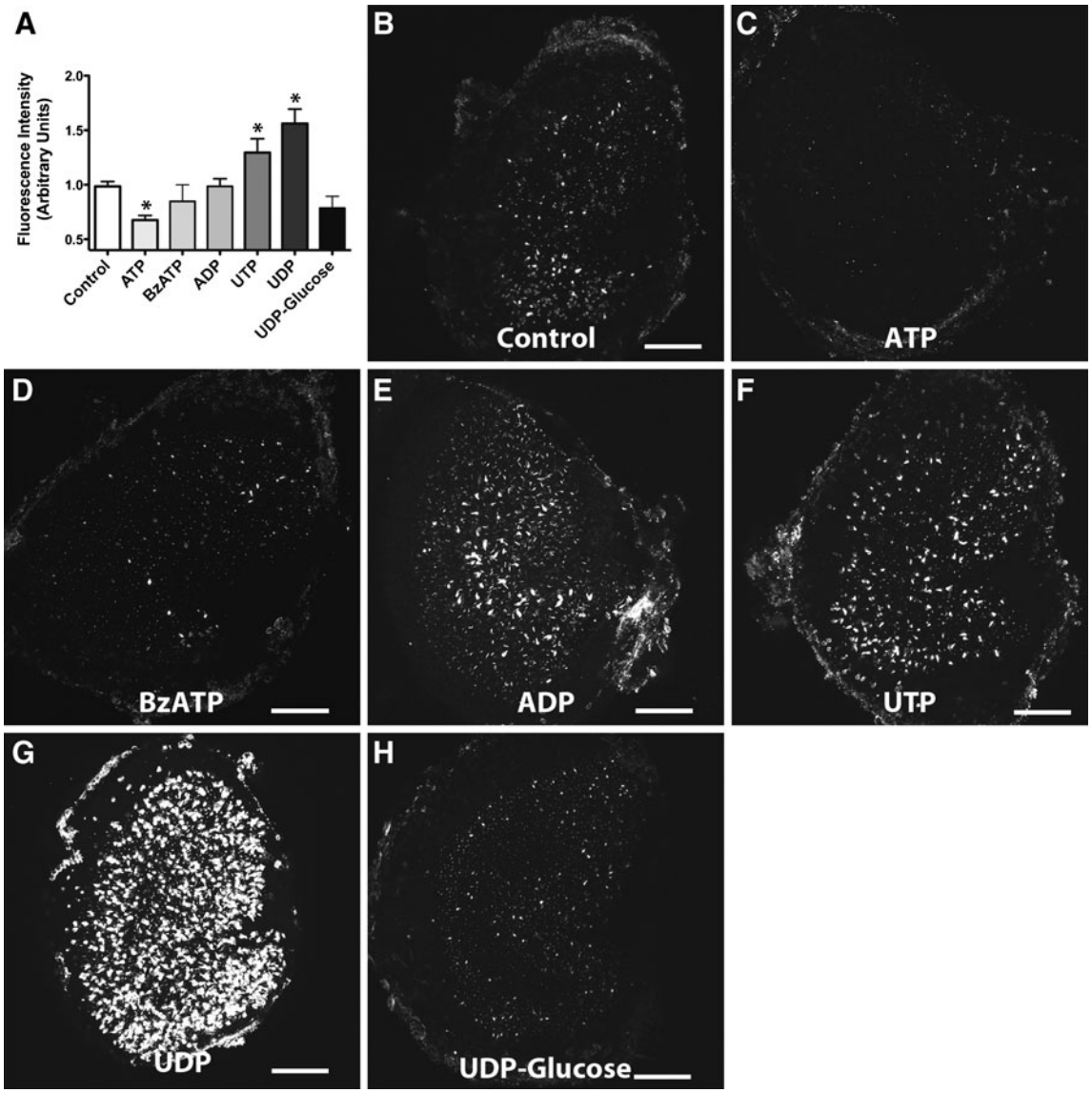

FIG. 7. Effects of P2 receptor agonists on fluorophore-conjugated phalloidin permeation **A** Mean fluorescent intensity of phalloidin-CF488A detected after pretreating with the various P2 receptor agonists. Shown are example maximum intensity Z-projection images of control (n=21) **(B)**, ATP (n=12) **(C)**, BzATP (n=9) **(D)**, ADP (n=11) **(E)**, UTP (n=11) **(F),** UDP (n=6) **(G),** and UDP-glucose (n=4) **(H)** treated utricles. Both UTP and UDP significantly enhanced uptake of phalloidin-CF488A (one-way ANOVA with Newman-Keuls multiple comparisons post-test, $p<0.05$) and ATP significantly blocked phalloidin-CF488A entry (one-way ANOVA with Newman-Keuls multiple comparisons post-test, $p<0.05$). Scale *bars* are 100 μm.

nM previously reported for this inhibitor in rats (Mamedova et al. 2004). We suspect that other P2Y receptors may be involved in the permeation, such as P2Y2, which also is responsive to uridine nucleotides and is expressed in the utricle sensory epithelium.

P2Y6, along with P2Y1, P2Y2, P2Y4, and P2Y11, can bind to $G_{q/11}$ to activate protein kinase C (PKC) via phospholipase C (PLC) (Burnstock 2004; Jacobson and Boeynaems 2010). To determine whether PLC-PKC signaling is involved downstream of P2Y activation in the permeation of phalloidin-CF488A, we examined the effects of U-73122, a PLC inhibitor, and BIM II, a PKC inhibitor, on phalloidin-CF488A entry. We also tested whether these antagonists would decrease phalloidin-CF488A uptake in the presence of the agonist, UDP. Fluorescence was decreased 37.5 % in the presence of U-73122 (One-way ANOVA with Newman-Keuls Multiple Comparisons Test, $p<0.05$, Fig. 8C; n=5). Additionally, BIM II treatments decreased fluorescence by 41.5 % (One-way ANOVA with

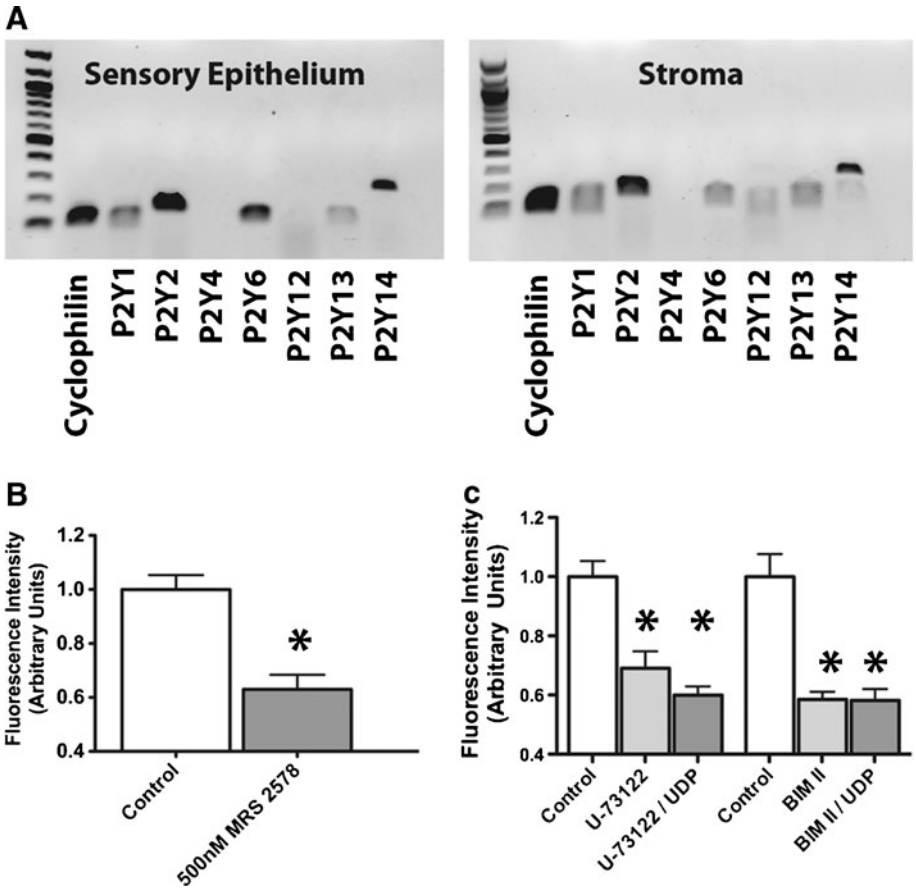

FIG. 8. P2Y receptor subunit expression and effects of P2Y6, PLC, and PKC inhibitors on fluorophore-conjugated phalloidin uptake (**A**) RT-PCR amplification of P2Y receptors in the sensory epithelium and stroma of P5 mouse utricles. The 100 bp ladder shown. **B** 500 nM MRS 2578, a P2Y6 receptor antagonist, decreased fluorophore-conjugated phalloidin uptake (n=4). **C** Summary of effect of U-73122 (PLC antagonist) and BIM II (PKC antagonist) on phalloidin-CF488A permeation. We observed decreased fluorescence from phalloidin-CF488A treatment in utricles treated with 10 μM U-73122 (n=5) or 50 μM BIM II (n=6). Utricles treated with UDP and either U-73122 (n=4) or BIM II (n=4) also had significantly decreased fluorescence compared with controls.

Newman-Keuls Multiple Comparisons Test, $p<0.05$, Fig. 8C; n=6). There also was decreased fluorescence in U-73122 and BIM II treated utricles that were additionally treated with UDP (One-way ANOVA with Newman-Keuls Multiple Comparisons Test, $p<0.05$, n=4).

The effectiveness of PPADS and suramin in blocking phalloidin uptake (Fig. 6B, E), together with the potency of UDP and UTP in stimulating phalloidin uptake (Fig. 7A, F, G), and the effectiveness of MRS 2578, U-73122, and BIM II in decreasing phalloidin-CF488A labeling (Fig. 8B, C), implicate

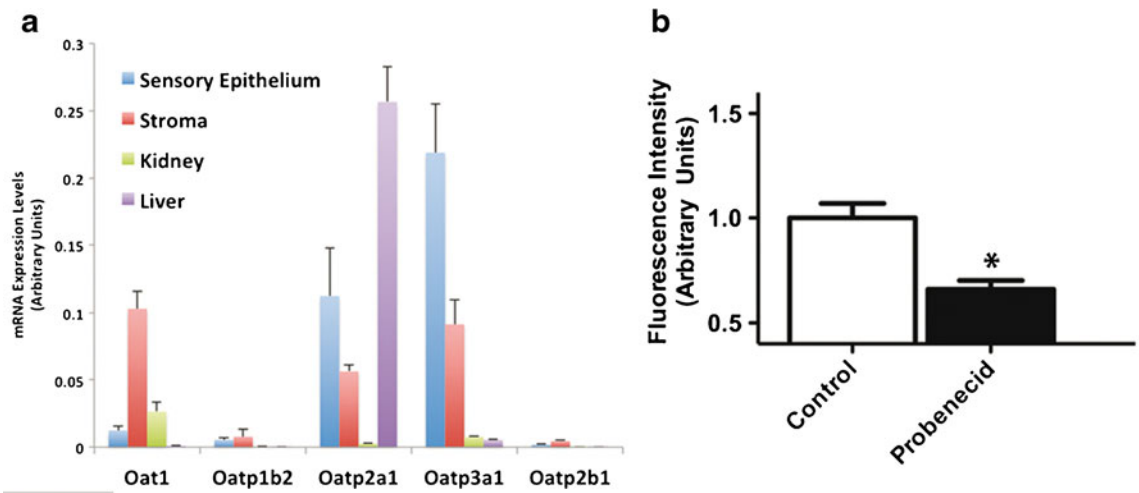

FIG. 9. Mouse utricle expresses Oat1 and Oatps. **A** mRNA expression levels of four Oatps, including *Oatp1b2*, which mediates phalloidin uptake in rodent hepatocytes, and *Oat1* in the neonatal mouse sensory epithelium, stroma, liver, and kidneys (n=3). **B** Probenecid treatments decreased fluorescence by 33.9 %.

P2Y-PLC-PKC signaling in the permeation of phalloidin into the neonatal mouse utricle.

Evaluation of OATPs in the permeation of phalloidin in the inner ear

The plasma membrane anionic transporters (OATs) and organic anion transporting polypeptides (OATPs) are transmembrane proteins capable of transporting diverse organic compounds (Obaidat et al. 2012; Roth et al. 2012). Phalloidin permeates hepatocytes through OATPs (Fehrenbach et al. 2003; Meier-Abt et al. 2004). Eleven OATPs and ten OATs have been discovered in a diversity of human tissues. To evaluate the potential roles of OATPs or OATs in the permeation of phalloidin in the inner ear, we measured the levels of expression for a subset of these transporters in the neonatal maculae, and compared them to the expression levels in the underlying stroma, the kidney, and the liver. We quantified mRNA expression for *Oat1, Oatp2b1, Oatp2a1, Oatp3a1,* and *Oatp1b2,* which is the OATP that allows rodent hepatocytes to take up phalloidin (Cihlar et al. 1999; Fehrenbach et al. 2003; Meier-Abt et al. 2004). We detected *Oat1, Oatp2a1,* and *Oatp3a1* expression in the maculae (Fig. 9A; n=3). There was 40.9-fold more *Oatp3a1* expression in the maculae than in the liver, but the liver expressed 2.3-fold more *Oatp2a1* transcripts. Oat1 plays a key role in transporting anions in the kidney, where we found its expression to be 2.1- and 28.9-fold more abundant compared to the maculae and liver, respectively. We did not detect abundant expression of the liver-specific *Oatp1b2,* in the utricle, kidney, or liver.

In a pharmacological test for the involvement of OATs or OATPs in the permeation of phalloidin in the utricle, we used probenecid, which inhibits many OATs and OATPs (Sugiyama et al. 2001; Yasui-Furukori et al. 2005; Jorgensen et al. 2007; Silverman et al. 2008). Consistent with a potential involvement for OATPs or OATs in the permeation of phalloidin, probenecid significantly inhibited phalloidin permeation and decreased fluorescence by 33.9 % (Student's t-test, $t(16)$=3.472, p=0.0003, Fig. 9B, n=15). Future investigations into whether a specific OATP or OAT is required for phalloidin permeation in hair cells may clarify a role for these transporters.

Besides OATs and OATPs, probenecid also inhibits pannexin channels (Silverman et al. 2008; Sandilos and Bayliss 2012). Pannexins are transmembrane proteins closely related to the gap-junction forming connexins (Baranova et al. 2004). Also, P2 receptor coupling to pannexin channels can cause cellular permeability to large dye molecules (North 2002). We used the pannexin channel inhibitor, CBX, to evaluate a potential role for these channels in the uptake of phalloidin-CF488A (Locovei et al. 2006). We observed no significant differences in fluorescence after CBX treatments (Student's $t$test, $t(5)$= 0.4321, p=0.6837, n=4), suggesting that pannexins are not involved in the permeation of fluorophore-conjugated phalloidin.

DISCUSSION

Permeation of fluorophore-conjugated phalloidin requires P2 receptor signaling

Our main finding is that phalloidin-CF488A can permeate living cells of the mouse utricle. The number of fluorescently labeled supporting cells in phalloidin-CF488A-treated utricles increases over time as utricles are maintained in phalloidin-free medium. P2 receptor antagonists effectively block phalloidin's permeation into hair cells. We also found that permeation is stimulated with UTP and UDP pretreatments, which are nucleotide agonists for a subset of P2Y receptors. Additionally, specific P2Y6, phospholipase c (PLC), and protein kinase C (PKC) inhibitors decrease permeation, implicating P2Y-PLC–PKC signaling in the uptake of phalloidin-CF488A.

Hair cells can take up a diversity of compounds through multiple different permeation routes. Styryl dyes enter hair cells via the mechanotransduction channel, endocytotic vesicles, and P2X channels (Balak et al. 1990; Nishikawa and Sasaki 1996; Griesinger et al. 2002; Meyers et al. 2003; Griesinger et al. 2004; Marcotti et al. 2005; Kaneko et al. 2006; Crumling et al. 2009). Ototoxic aminoglycosides also enter hair cells through multiple routes including the mechanotransduction channel, endocytosis, chloride/bicarbonate exchangers, and TRPA1 channels (Alharazneh et al. 2011; Stepanyan et al. 2011; Hailey et al. 2012). This is the first reported evidence of living hair cells taking up phalloidin.

Unlike styryl dyes, we did not observe rapid uptake of phalloidin-CF488A into hair cells. Phalloidin-CF488A entered a subset of hair cells after 20 min, but robust phalloidin permeation and fluorescent labeling did not occur until we incubated utricles for longer durations. We found that permeation required metabotropic P2Y and PLC-PKC second messenger signaling, which might explain why the permeation is not rapid. As P2Y receptors are not pore-forming, the route of permeation route is unknown, although OATPs are a likely possibility.

Liver-specific OATPs mediate the permeation of phalloidin into hepatocytes (Fehrenbach et al. 2003; Meier-Abt et al. 2004). Organic anion transporter

polypeptides mediate sodium-independent transport of a wide diversity of organic compounds, and currently 11 human OATP proteins have been described (Hagenbuch and Meier 2004; Roth et al. 2012). Rodent Oatp1b2 and human OATP1B1 and OATP1B3 enable phalloidin uptake into hepatocytes (Fehrenbach et al. 2003; Meier-Abt et al. 2004; Lu et al. 2008). OATs, similar to OATPs, mediate transport of organic compounds, although with smaller molecular weights (VanWert et al. 2010).

Several lines of evidence suggest an involvement of OATs or OATPs in the permeation of phalloidin into hair cells. First, we found that an OATP and OAT antagonist, probenecid, decreased phalloidin permeation. Second, we detected mRNA expression of *Oat1* and some OATPs in the sensory epithelium. Our investigation is limited since we did not examine and compare the expression levels for all 15 rodent OATP genes. We only sought to discover whether the neonatal mouse maculae expressed OATPs. We did not discover *Oatp1b2* expression in the utricle, which is the transporter that mediates hepatocellular phalloidin uptake. Thirdly, second messenger systems, including PKC, can regulate OATP transport activity (Kock et al. 2010; Roth et al. 2012). P2Y6 activates a phosphatidylinositol-calcium second messenger system leading to PKC activation (Kim et al. 2003). We discovered decreased phalloidin-CF488A labeling with PLC and PKC antagonists, which lends support to a potential requirement for second messenger signaling in the permeation of phalloidin in HCs. Future investigations into the expression pattern and localizations of specific OATPs may provide insight into a potential role for these transporters in the uptake of phalloidin into hair cells.

It appears that second messenger signaling pathways under the regulation from P2Y receptors control the expression and activity of OATPs to mediate phalloidin uptake into hair cells. Many different organic compounds are transported through OATPs. Although we have seen no evidence, it remains possible that aminoglycosides, which are ototoxic and nephrotoxic, could enter hair cells through this mechanism.

Evidence for supporting cell coupling within sensory epithelium

When phalloidin-treated utricles were cultured 24 h in phalloidin-free media after washout, the fluorescent label disappeared from HCs and appeared in the supporting cells. Supporting cells in the vestibular epithelia and the organ of Corti are coupled through gap junctions formed by connexins (Santos-Sacchi and Dallos 1983; Sato and Santos-Sacchi 1994; Zhao and Santos-Sacchi 2000; Forge et al. 2003; Zhang et al. 2005; Jagger and Forge 2006; Zhu and Zhao 2010). Connexins are expressed in the supporting cells of all mouse vestibular epithelia (Forge et al. 2003; Qu et al. 2007). Gap junctions form channels in the membrane of a cell in register with the membrane of a neighboring cell and allow for direct communication between the cells. This coupling is required for normal HC physiology and K^+ recycling (Wangemann 2002). Phalloidin became localized throughout the supporting cells 24 h after the label was washed out, and it is possible that it diffuses through the gap junction-coupled supporting cell network.

We did not investigate how phalloidin permeated into the supporting cells, whether phalloidin was directly transferred from neighboring hair cells or whether supporting cells took it up through the extracellular media. Supporting cells possess unpaired plasma membrane connexin hemichannels that can take in anionic molecules (Zhao 2005). It remains possible that hair cells transfer the phalloidin to the neighboring supporting cells, and then the phalloidin freely transfers throughout the coupled supporting cells.

Potential applications of fluorophore-conjugated phalloidin labeling inner ear hair cells

The permeation of fluorophore-conjugated phalloidin into cells of the inner ear provides a novel mechanism to vitally label sensory hair cells. Phalloidin has high affinity for filamentous actin ($Kd=3.6\times10^{-8}$) (Wieland et al. 1975; Faulstich et al. 1977). Upon permeating hair cells, it specifically labels F-actin-rich cellular structures, including stereocilia, and cuticular plates. Due to phalloidin's affinity for F-actin, it is useful for investigating retrograde F-actin flow and the coordination between the actin and microtubules cytoskeletal networks advancing growth cones and neurites (Schaefer et al. 2002; Burnette et al. 2007, 2008; Schaefer et al. 2008). If a low enough concentration of fluorophore-conjugated phalloidin is introduced into HCs, this could provide a new method for analyzing retrograde actin flow in HCs and treadmilling rates within stereocilia (Schneider et al. 2002; Zhang et al. 2012).

In summary, we have found that fluorophore-conjugated phalloidin permeates living hair cells of the mouse utricle and that this requires activation of P2Y receptors and appears to work through PLC–PKC second messenger signaling. In the 24 h after washout of the label in culture, the fluorescence gradually disappears from HCs and increases in the neighboring SCs. The implications of our results may be useful for live cell imaging and the study of actin dynamics in hair cell epithelia.

ACKNOWLEDGMENTS

We thank Jeffrey Holt for helpful advice, discussion, and technical assistance. We thank Douglas Bayliss for discussion and critical comments. This work was supported by grants from the National Institutes of Health DC000200 (J.T.C), DC012485 (B.R.T), and T32 GM007055 (B.R.T), and the Lions of Virginia Hearing Research Foundation (J.T.C).

Conflict of Interest Authors declare that they have no conflict of interest.

REFERENCE

ALHARAZNEH A, LUK L, HUTH M, MONFARED A, STEYGER PS, CHENG AG, RICCI AJ (2011) Functional hair cell mechanotransducer channels are required for aminoglycoside ototoxicity. PLoS One 6:e22347

BALAK KJ, CORWIN JT, JONES JE (1990) Regenerated hair cells can originate from supporting cell progeny: evidence from phototoxicity and laser ablation experiments in the lateral line system. J Neurosci 10:2502–2512

BARANOVA A, IVANOV D, PETRASH N, PESTOVA A, SKOBLOV M, KELMANSON I, SHAGIN D, NAZARENKO S, GERAYMOVYCH E, LITVIN O, TIUNOVA A, BORN TL, USMAN N, STAROVEROV D, LUKYANOV S, PANCHIN Y (2004) The mammalian pannexin family is homologous to the invertebrate innexin gap junction proteins. Genomics 83:706–716

BURNETTE DT, SCHAEFER AW, JI L, DANUSER G, FORSCHER P (2007) Filopodial actin bundles are not necessary for microtubule advance into the peripheral domain of *Aplysia* neuronal growth cones. Nat Cell Biol 9:1360–1369

BURNETTE DT, JI L, SCHAEFER AW, MEDEIROS NA, DANUSER G, FORSCHER P (2008) Myosin II activity facilitates microtubule bundling in the neuronal growth cone neck. Dev Cell 15:163–169

BURNS JC, ON D, BAKER W, COLLADO MS, CORWIN JT (2012) Over half the hair cells in the mouse utricle first appear after birth, with significant numbers originating from early postnatal mitotic production in peripheral and striolar growth zones. J Assoc Res Otolaryngol 13:609–627

BURNSTOCK G (2004) Introduction: P2 receptors. Curr Top Med Chem 4:793–803

CANKURTARAN-SAYAR S, SAYAR K, UGUR M (2009) P2X7 receptor activates multiple selective dye-permeation pathways in RAW 264.7 and human embryonic kidney 293 cells. Mol Pharmacol 76:1323–1332

CIHLAR T, LIN DC, PRITCHARD JB, FULLER MD, MENDEL DB, SWEET DH (1999) The antiviral nucleotide analogs cidofovir and adefovir are novel substrates for human and rat renal organic anion transporter 1. Mol Pharmacol 56:570–580

COLUCCIO LM, TILNEY LG (1984) Phalloidin enhances actin assembly by preventing monomer dissociation. J Cell Biol 99:529–535

CRUMLING MA, TONG M, ASCHENBACH KL, LIU LQ, PIPITONE CM, DUNCAN RK (2009) P2X antagonists inhibit styryl dye entry into hair cells. Neuroscience 161:1144–1153

DANCKER P, LÖW I, HASSELBACH W, WIELAND T (1975) Interaction of actin with phalloidin: polymerization and stabilization of F-actin. Biochim Biophys Acta 400:407–414

ESTES JE, SELDEN LA, GERSHMAN LC (1981) Mechanism of action of phalloidin on the polymerization of muscle actin. Biochemistry 20:708–712

FAULSTICH H, SCHAFER AJ, WECKAUF M (1977) The dissociation of the phalloidin-actin complex. Hoppe Seylers Z Physiol Chem 358:181–184

FAULSTICH H, TRISCHMANN H, MAYER D (1983) Preparation of tetramethylrhodaminyl-phalloidin and uptake of the toxin into short-term cultured hepatocytes by endocytosis. Exp Cell Res 144:73–82

FEHRENBACH T, CUI Y, FAULSTICH H, KEPPLER D (2003) Characterization of the transport of the bicyclic peptide phalloidin by human hepatic transport proteins. Naunyn Schmiedeberg's Arch Pharmacol 368:415–420

FORGE A, BECKER D, CASALOTTI S, EDWARDS J, MARZIANO N, NEVILL G (2003) Gap junctions in the inner ear: comparison of distribution patterns in different vertebrates and assessement of connexin composition in mammals. J Comp Neurol 467:207–231

FRIMMER M, PETZINGER E, ZIEGLER K, VEIL LB (1980) Uptake of 3H-demethylphalloin by isolated hepatocytes in the presence of various concentrations of phalloin or phalloidin. Naunyn Schmiedebergs Arch Pharmacol 311:91–94

GALE JE, MARCOTTI W, KENNEDY HJ, KROS CJ, RICHARDSON GP (2001) FM1-43 dye behaves as a permeant blocker of the hair-cell mechanotransducer channel. J Neurosci 21:7013–7025

GRIESINGER CB, RICHARDS CD, ASHMORE JF (2002) Fm1-43 reveals membrane recycling in adult inner hair cells of the mammalian cochlea. J Neurosci 22:3939–3952

GRIESINGER CB, RICHARDS CD, ASHMORE JF (2004) Apical endocytosis in outer hair cells of the mammalian cochlea. Eur J Neurosci 20:41–50

HAGENBUCH B, MEIER PJ (2004) Organic anion transporting polypeptides of the OATP/ SLC21 family: phylogenetic classification as OATP/ SLCO superfamily, new nomenclature and molecular/ functional properties. Pflugers Arch 447:653–665

HAILEY DW, ROBERTS B, OWENS KN, STEWART AK, LINBO T, PUJOL R, ALPER SL, RUBEL EW, RAIBLE DW (2012) Loss of Slc4a1b chloride/bicarbonate exchanger function protects mechanosensory hair cells from aminoglycoside damage in the zebrafish mutant persephone. PLoS Genetics 8:e1002971

HOUSLEY GD (1998) Extracellular nucleotide signaling in the inner ear. Mol Neurobiol 16:21–48

HOUSLEY G, GALE J (2010) Purinergic signalling in the inner ear-perspectives and progress. Purinergic Signal 6:151–153

HOUSLEY GD, GREENWOOD D, ASHMORE JF (1992) Localization of cholinergic and purinergic receptors on outer hair cells isolated from the guinea-pig cochlea. Proc Biol Sci 249:265–273

HOUSLEY GD, LUO L, RYAN AF (1998) Localization of mRNA encoding the P2X2 receptor subunit of the adenosine 5′-triphosphate-gated ion channel in the adult and developing rat inner ear by in situ hybridization. J Comp Neurol 393:403–414

HOUSLEY GD, KANJHAN R, RAYBOULD NP, GREENWOOD D, SALIH SG, JÄRLEBARK L, BURTON LD, SETZ VC, CANNELL MB, SOELLER C, CHRISTIE DL, USAMI S, MATSUBARA A, YOSHIE H, RYAN AF, THORNE PR (1999) Expression of the P2X(2) receptor subunit of the ATP-gated ion channel in the cochlea: implications for sound transduction and auditory neurotransmission. J Neurosci 19:8377–8388

HOUSLEY GD, BRINGMANN A, REICHENBACH A (2009) Purinergic signaling in special senses. Trends Neurosci 32:128–141

HUANG LC, THORNE PR, VLAJKOVIC SM, HOUSLEY GD (2010) Differential expression of P2Y receptors in the rat cochlea during development. Purinergic Signal 6:231–248

JACOBSON KA, BOEYNAEMS JM (2010) P2Y nucleotide receptors: promise of therapeutic applications. Drug Discov Today 15:570–578

JAGGER DJ, FORGE A (2006) Compartmentalized and signal-selective gap junctional coupling in the hearing cochlea. J Neurosci Off J Soc Neurosci 26:1260–1268

Jorgensen JM (1989) Evolution of octavolarteralis sensory cells. In: Coombs S, Gorner P, Munz H (eds) The mechanosensory lateral line: neurobiology and evolution. Springer-Verlag, New York, p 115–145

Jorgensen L, Van Beek J, Lund S, Schousboe A, Badolo L (2007) Evidence of Oatp and Mdr1 in cryopreserved rat hepatocytes. European Journal of Pharmaceutical Sciences: Official Journal of the European Federation for Pharmaceutical Sciences 30:181–189

Kaneko T, Harasztosi C, Mack AF, Gummer AW (2006) Membrane traffic in outer hair cells of the adult mammalian cochlea. Eur J Neurosci 23:2712–2722

Kawashima Y, Géléoc GS, Kurima K, Labay V, Lelli A, Asai Y, Makishima T, Wu DK, Della Santina CC, Holt JR, Griffith AJ (2011) Mechanotransduction in mouse inner ear hair cells requires transmembrane channel-like genes. J Clin Invest 121:4796–4809

Kennedy C, Qi AD, Herold CL, Harden TK, Nicholas RA (2000) ATP, an agonist at the rat P2Y(4) receptor, is an antagonist at the human P2Y(4) receptor. Mol Pharmacol 57:926–931

Kim SG, Gao ZG, Soltysiak KA, Chang TS, Brodie C, Jacobson KA (2003) P2Y6 nucleotide receptor activates PKC to protect 1321N1 astrocytoma cells against tumor necrosis factor-induced apoptosis. Cell Mol Neurobiol 23:401–418

Kock K, Koenen A, Giese B, Fraunholz M, May K, Siegmund W, Hammer E, Volker U, Jedlitschky G, Kroemer HK, Grube M (2010) Rapid modulation of the organic anion transporting polypeptide 2B1 (OATP2B1, SLCO2B1) function by protein kinase C-mediated internalization. J Biol Chem 285:11336–11347

Lambrecht G, Friebe T, Grimm U, Windscheif U, Bungardt E, Hildebrandt C, Baumert HG, Spatz-Kumbel G, Mutschler E (1992) PPADS, a novel functionally selective antagonist of P2 purinoceptor-mediated responses. Eur J Pharmacol 217:217–219

Lambrecht G, Braun K, Damer M, Ganso M, Hildebrandt C, Ullmann H, Kassack MU, Nickel P (2002) Structure-activity relationships of suramin and pyridoxal-5′-phosphate derivatives as P2 receptor antagonists. Curr Pharm Des 8:2371–2399

Li C (2000) Novel mechanism of inhibition by the P2 receptor antagonist PPADS of ATP-activated current in dorsal root ganglion neurons. J Neurophysiol 83:2533–2541

Lin CH, Forscher P (1995) Growth cone advance is inversely proportional to retrograde F-actin flow. Neuron 14:763–771

Locovei S, Bao L, Dahl G (2006) Pannexin 1 in erythrocytes: function without a gap. Proc Natl Acad Sci U S A 103:7655–7659

Lu H, Choudhuri S, Ogura K, Csanaky IL, Lei X, Cheng X, Song PZ, Klaassen CD (2008) Characterization of organic anion transporting polypeptide 1b2-null mice: essential role in hepatic uptake/toxicity of phalloidin and microcystin-LR. Toxicol Sci 103:35–45

Mamedova LK, Joshi BV, Gao ZG, von Kügelgen I, Jacobson KA (2004) Diisothiocyanate derivatives as potent, insurmountable antagonists of P2Y6 nucleotide receptors. Biochem Pharmacol 67:1763–1770

Marcotti W, van Netten SM, Kros CJ (2005) The aminoglycoside antibiotic dihydrostreptomycin rapidly enters mouse outer hair cells through the mechano-electrical transducer channels. J Physiol 567:505–521

Meier-Abt F, Faulstich H, Hagenbuch B (2004) Identification of phalloidin uptake systems of rat and human liver. Biochim Biophys Acta 1664:64–69

Meyers JR, MacDonald RB, Duggan A, Lenzi D, Standaert DG, Corwin JT, Corey DP (2003) Lighting up the senses: FM1-43 loading of sensory cells through nonselective ion channels. J Neurosci 23:4054–4065

Munter K, Mayer D, Faulstich H (1986) Characterization of a transporting system in rat hepatocytes. Studies with competitive and non-competitive inhibitors of phalloidin transport. Biochimica et Biophysica Acta 860:91–98

Nishikawa S, Sasaki F (1996) Internalization of styryl dye FM1-43 in the hair cells of lateral line organs in *Xenopus* larvae. The journal of histochemistry and cytochemistry : official journal of the Histochemistry Society 44:733–741

North RA (2002) Molecular physiology of P2X receptors. Physiol Rev 82:1013–1067

Obaidat A, Roth M, Hagenbuch B (2012) The expression and function of organic anion transporting polypeptides in normal tissues and in cancer. Annu Rev Pharmacol Toxicol 52:135–151

Petzinger, E. & Frimmer, M. (1988) Comparative investigations on the uptake of phaliotoxins, bile acids, bovine lactoperoxidase and horseradish peroxidase into rat hepatocytes in suspension and in cell cultures. Biochimica et Biophysica Acta 135–144.

Qu Y, Tang W, Dahlke I, Ding D, Salvi R, Sohl G, Willecke K, Chen P, Lin X (2007) Analysis of connexin subunits required for the survival of vestibular hair cells. J Comp Neurol 504:499–507

Roth M, Obaidat A, Hagenbuch B (2012) OATPs, OATs and OCTs: the organic anion and cation transporters of the SLCO and SLC22A gene superfamilies. Br J Pharmacol 165:1260–1287

Saffer LD, Gu R, Corwin JT (1996) An RT-PCR analysis of mRNA for growth factor receptors in damaged and control sensory epithelia of rat utricles. Hear Res 94:14–23

Sandilos JK, Bayliss DA (2012) Physiological mechanisms for the modulation of pannexin 1 channel activity. J Physiol 590:6257–6266

Santos-Sacchi J, Dallos P (1983) Intercellular communication in the supporting cells of the organ of Corti. Hear Res 9:317–326

Sato Y, Santos-Sacchi J (1994) Cell coupling in the supporting cells of Corti's organ: sensitivity to intracellular H+and Ca+2. Hear Res 80:21–24

Schaefer AW, Kabir N, Forscher P (2002) Filopodia and actin arcs guide the assembly and transport of two populations of microtubules with unique dynamic parameters in neuronal growth cones. J Cell Biol 158:139–152

Schaefer AW, Schoonderwoert VT, Ji L, Mederios N, Danuser G, Forscher P (2008) Coordination of actin filament and microtubule dynamics during neurite outgrowth. Dev Cell 15:146–162

Schneider ME, Belyantseva IA, Azevedo RB, Kachar B (2002) Rapid renewal of auditory hair bundles. Nature 418:837–838

Silverman W, Locovei S, Dahl G (2008) Probenecid, a gout remedy, inhibits pannexin 1 channels. Am J Physiol Cell Physiol 295: C761–C767

Stepanyan RS, Indzhykulian AA, Vélez-Ortega AC, Boger ET, Steyger PS, Friedman TB, Frolenkov GI (2011) TRPA1-mediated accumulation of aminoglycosides in mouse cochlear outer hair cells. J Assoc Res Otolaryngol 12:729–740

Sugiyama D, Kusuhara H, Shitara Y, Abe T, Meier PJ, Sekine T, Endou H, Suzuki H, Sugiyama Y (2001) Characterization of the efflux transport of 17beta-estradiol-D-17beta-glucuronide from the brain across the blood–brain barrier. J Pharmacol Exp Ther 298:316–322

Surprenant A, Rassendren F, Kawashima E, North RA, Buell G (1996) The cytolytic P2Z receptor for extracellular ATP identified as a P2X receptor (P2X7). Science 272:735–738

Surprenant A, Schneider DA, Wilson HL, Galligan JJ, North RA (2000) Functional properties of heteromeric P2X(1/5) receptors expressed in HEK cells and excitatory junction potentials in guinea-pig submucosal arterioles. J Auton Nerv Syst 81:249–263

Szücs A, Szappanos H, Tóth A, Farkas Z, Panyi G, Csernoch L, Sziklai I (2004) Differential expression of purinergic receptor subtypes in the outer hair cells of the guinea pig. Hear Res 196:2–7

Trujillo CA, Nery AA, Martins AH, Majumder P, Gonzalez FA, Ulrich H (2006) Inhibition mechanism of the recombinant rat P2X(2) receptor in glial cells by suramin and TNP-ATP. Biochem 45:224–233

VANWERT AL, GIONFRIDDO MR, SWEET DH (2010) Organic anion transporters: discovery, pharmacology, regulation and roles in pathophysiology. Biopharm Drug Dispos 31:1–71

WALLI AK, WIELAND E, WIELAND T (1981) Phalloidin uptake by the liver of cholestatic rats in vivo, in isolated perfused liver and isolated hepatocytes. Naunyn Schmiedebergs Arch Pharmacol 316:257–261

WANGEMANN P (2002) K+cycling and the endocochlear potential. Hear Res 165:1–9

WATERMAN-STORER CM, DESAI A, BULINSKI JC, SALMON ED (1998) Fluorescent speckle microscopy, a method to visualize the dynamics of protein assemblies in living cells. Curr Biol 8:1227–1230

WIELAND T, DE VRIES JX, SCHÄFER A, FAULSTICH H (1975) Spectroscopic evidence for the interaction of phalloidin with actin. FEBS Lett 54:73–75

YASUI-FURUKORI N, UNO T, SUGAWARA K, TATEISHI T (2005) Different effects of three transporting inhibitors, verapamil, cimetidine, and probenecid, on fexofenadine pharmacokinetics. Clin Pharmacol Ther 77:17–23

ZHANG Y, TANG W, AHMAD S, SIPP JA, CHEN P, LIN X (2005) Gap junction-mediated intercellular biochemical coupling in cochlear supporting cells is required for normal cochlear functions. Proc Natl Acad Sci U S A 102:15201–15206

ZHANG DS, PIAZZA V, PERRIN BJ, RZADZINSKA AK, POCZATEK JC, WANG M, PROSSER HM, ERVASTI JM, COREY DP, LECHENE CP (2012) Multi-isotope imaging mass spectrometry reveals slow protein turnover in hair-cell stereocilia. Nature 481:520–524

ZHAO HB (2005) Connexin26 is responsible for anionic molecule permeability in the cochlea for intercellular signalling and metabolic communications. Eur J Neurosci 21:1859–1868

ZHAO S, FERNALD RD (2005) Comprehensive algorithm for quantitative real-time polymerase chain reaction. J Comput Biol 12:1047–1064

ZHAO HB, SANTOS-SACCHI J (2000) Voltage gating of gap junctions in cochlear supporting cells: evidence for nonhomotypic channels. J Membr Biol 175:17–24

ZHU Y, ZHAO HB (2010) ATP-mediated potassium recycling in the cochlear supporting cells. Purinergic Signaling 6:221–229